MEANDROS MEDICAL AND DENTAL JOURNAL
March 2025 (1): 12-18

Meandros Medical and Dental Journal
doi: 10.69601/meandrosmdj.1591566

Research Article

DETECTION OF *Staphylococcus aureus* VIA APTAMER-GATED MCM-41 NANOPARTICLES

Samet UÇAK*

Department of Medical Biology, Medical Faculty, Istanbul Aydin University, Istanbul, Turkiye
*Correspondence: sametucak@aydin.edu.tr

Received: *26 November 2025*
Revised: *27 February 2025*
Accepted: *03 March 2025*
Published: *20 March 2025*

ABSTRACT

Objective: Aptamer-gated nanoparticles are a possible way to find *Staphylococcus aureus* because they are very specific, sensitive, and quick to detect.

Materials and Methods: MCM-41 nanoparticles were characterized via DLS, SEM, and FTIR techniques. Reference strains *S. aureus*, *S. epidermidis*, and *Escherichia coli* were used. After the synthesis of the fluorescence-loaded silica-coated MCM-41 nanoparticles, fluorescence release experiments were performed via a dialysis membrane.

Results: The particle size of the MCM-41 nanoparticles was determined to be 192 ±1.782 nm. BET analysis revealed that each MCM-41 particle had a specific surface area of 1019.37 m^2/g, pores that were 2.42 nm wide, and the ability to hold 0.99 cm^3/g of material. The MCM-41 nanoparticles were nanosized, had a narrow size distribution, and were smooth, amorphous and spherical in shape. Amino group-functionalized MCM-41 nanoparticles via the APTES reaction. FT-IR analysis was performed to determine the correct conjugation. After the addition of amino acids, typical bands at 690 and 1460 nm appeared. These bands correspond to N–H bending vibrations and N–H asymmetric bending vibrations, respectively. The fluorescein-loaded silica particles conjugated with the aptamer and the target bacterium *S. aureus* had the maximum release. Furthermore, approximately 70% fluorescein release occurred within 6 hours. It was possible to quickly and accurately find *S. aureus* at detection limits as low as 164 CFU/mL in PBS.

Conclusion: The proposed biosensor has many benefits, such as quick response times, high sensitivity, and specificity for *S. aureus* detection. Future studies will likely concentrate on increasing the sensitivity of these technologies, decreasing detection times, and broadening their range of applications.

Keywords: Aptamer, Biosensor, MCM-41 nanoparticle, *S. aureus*, Specific detection.

MEANDROS MEDICAL AND DENTAL JOURNAL
March 2025 (1): 12-18

Meandros Medical and Dental Journal
doi: 10.69601/meandrosmdj.1591566

INTRODUCTION

In recent years, the rapid and sensitive detection of bacterial pathogens has become increasingly important in various disciplines, including health care, food safety, and environmental monitoring. *Staphylococcus aureus* (*S. aureus*) is a notable pathogen because of its capacity to induce various infections, ranging from superficial skin conditions to severe, life-threatening illnesses (1). One of the most clinically significant species is the *S. aureus* bacterium. *S. aureus*, which has a gram-positive coccus morphology, is highly adaptable in terms of its ability to acquire resistance to antibiotics. When faced with novel obstacles, *S. aureus* adapts quickly, which aids in its survival and clonal growth (2, 3). Information reported in 2019 by the U.S. Centers for Disease Control and Prevention (CDC), on the basis of 2017 data, revealed that *S. aureus* infections in the U.S. infected 119,000 people and caused the deaths of approximately 20,000 people, highlighting it as a major problem (4). To address the need for efficient detection methods, biosensors have emerged as promising tools for the rapid and specific detection of bacterial pathogens (5).

MCM-41 is a type of mesoporous silica material with a hexagonal array of uniform pores. Recent studies have highlighted the versatility of MCM-41 in various applications, particularly in catalysis and drug delivery. For example, its high surface area and tunable pore size make it an excellent candidate for supporting catalysts in chemical reactions, leading to enhanced reaction rates and selectivity (6, 7). MCM-41 is also biocompatible and can encapsulate a wide range of drugs. This makes it a promising material in the field of nanomedicine for targeted drug delivery systems that improve the effectiveness and controlled release of therapeutics (8).

The active targeting of nanoparticulate systems frequently involves the use of aptamers (9). Aptamers are single-stranded nucleic acids that are synthetically produced under in vitro conditions. These synthetic oligonucleotides can bind to a wide variety of target molecules (proteins, metal ions, monosaccharides, peptides, microorganisms, cells, and tissues) with high selectivity and affinity. DNA or RNA can be composed of aptamers. Their specific binding to target molecules occurs due to their three-dimensional structures. Aptamers can be easily modified to target specific molecules (10-12). Owing to their low molecular weight, ease of repeated synthesis, nontoxic nature as targeting ligands, and ability to regain their active conformation, aptamers have advantages in active targeting. In addition to their use as biosensors, active targeting systems utilize aptamers for diagnosis, treatment, and drug delivery (13).

This paper introduces a biosensor utilizing aptamer-functionalized MCM-41 for the quick and highly sensitive detection of S. aureus.

MATERIALS AND METHODS

All additional compounds, including 3-(triethoxysilyl)-propylamine (APTES) and MCM-41, were acquired from Sigma-Aldrich. The *S. aureus* oligonucleotide was synthesized by Sentegen (Ankara, Türkiye). In accordance with the sequence published by Cao and colleagues (14), the *S. aureus* binding aptamer was synthesized as follows: 5′ amino-labeled aptamer sequence (5′-GCG CCC TCT CAC GTG GCA CTC AGA GTG CCG GAA GTT CTG CGT TAT-3′). The reference strains *S. aureus* (ATCC 29213), *S. epidermidis* (ATCC 12228), and *Escherichia coli* (ATCC 25922) were obtained recently from the American Type Culture Collection (ATCC). Figure 1 is a schematic depiction of strategy as used in this study.

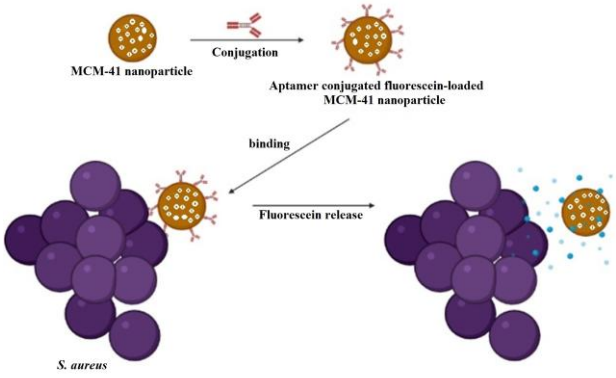

Figure 1. The general scheme of aptamer-gated specific fluorescein release profile approach.

Characterization of MCM-41 Nanoparticles

The particle sizes were measured with a Zetasizer ZEN 3600 Nano-ZS (Malvern Instruments, Worcestershire, UK). One milligram of MCM-41 particles was suspended in PBS and sonicated for 20 minutes in phosphate buffer (50 mM, pH 7.0) at room temperature to plot the intensity vs. diameter size.

The morphological evaluation of the particles was performed via Brunauer–Emmett–Teller (BET) (Quantachrome BET analyzer, Anton–Paar) and scanning electron microscopy (SEM; Zeiss EVO LS 10) at Yıldız Technical University's MERKLAB, Türkiye.
To determine whether amine groups were present on the surfaces of the MCM-41 nanoparticles, Fourier transform

infrared (FTIR) spectroscopy (Perkin Elmer Inc., Norwalk, CT, USA) fitted with a Universal ATR attachment was used. The one-bounce ATR mode was utilized to capture the ATR-FTIR spectra of the silica-coated magnetic nanoparticles. The spectral wavelengths ranged from 650 cm^{-1} to 4000 cm^{-1} when one milliliter of MCM-41 nanoparticle sample in PBS was used.

Aptamer-functionalized magnetic-silica particle preparation

The surface free amine groups of hybrid magnetic-silica particles were covalently linked with amino-modified aptamers after being initially activated with glutaraldehyde (15). Two hundred fifty milligrams of amino-functionalized hybrid magnetic-silica particles were introduced into a reactor containing 2% glutaraldehyde in 0.1 M phosphate buffer at pH 7.0. After the coupling reaction was conducted for 3h at 35°C, the mixture was subsequently rinsed with 0.1 M acetic acid, followed by 0.1 M phosphate buffer. Two hours after being placed in phosphate buffer at a concentration of 50 mM and a pH of 8.5, fifty milligrams of hybrid silica nanoparticles that were already functionalized with amino groups were transferred to phosphate buffer containing *S. aureus* binding aptamer at concentrations of 100 µL and 200 µM. An aptamer that was tagged with 5' amino acids was attached to magnetic beads at a temperature of 25°C for a period of 18h while the reaction mixture was continually mixed. Finally, the noncovalently attached aptamer molecules were extracted from the magnetic beads by using a buffer consisting of PBS. A UV–vis spectrophotometer (Agilent 8000, USA) was used to quantify the quantity of bound aptamer via the UV-absorption method at 265 nm.

Synthesis of silica coated MCM-41 nanoparticles

A previously presented approach (16) was employed to synthesize amino-functionalized SiO_2 nanoparticles. One milliliter of 95% ethanol, including 5% 1 mM acetic acid, was agitated with 50 mg of MCM-41 for 1h at room temperature. After adding the APTES solution at a molar ratio of MCM41/APTES (1/5) and mixing, the mixture was incubated overnight. The solution was rinsed three times with 1× PBS during centrifugation (14000 rpm, 5 min). Following the dissolution of 10 µl of amino-modified nanoparticles in 190 µl of 1× PBS, 100 µM fluorescein sodium salt was added. While the solution was stirred, it was incubated overnight. Finally, the fluorescein-loaded silica nanoparticles present in the PBS solution were conjugated with a 1 µM *S. aureus* 5' amino-labeled aptamer sequence. The solution was stirred while it was incubated overnight. By comparing the spectra of the initial and final concentrations (Ex: 460 nm, Em: 520 nm), the levels of fluorescein (FL) were quantified.

Bacterial cultures

S.aureus, *S. epidermidis*, and *E. coli* were grown overnight in tryptone soy broth (TSB) from frozen stocks at 37°C. To attain the desired concentrations, the cultures were serially diluted in PBS buffer. The individual colony-forming units (CFUs) were enumerated following the surface plating of samples on TSB agar plates, which were incubated 37°C overnight.

Fluorescence assay

The samples spiked with the specific bacteria were culture-plated for colony counting, and fluorescence was assayed after the addition of one milligram of aptamer-nanoparticles. Eluted cells were serially diluted on TSB agar plates and cultivated overnight at 37°C. The number of viable colonies was counted and reported as CFU/ml.

Fluorescence release experiments

A fluorescence spectrophotometer (Fluoromax 4, Horiba) with Ex. 460 nm and Em. 520 nm was used to measure the release of fluorescein molecules from pores. The coated mesoporous silica particles were placed in a cell holder. The particles were confined within a compartment formed by a dialysis membrane (molecular cutoff of 12,000 Da) at the top of the spectroscopic cuvette, thereby preventing their mixing, as previously documented (17). Throughout the readings, the mixture was constantly swirled to make it uniform. The samples were measured at different points in time. The cumulative fluorescein release as a percentage of total molecules was plotted.

RESULTS

The particle size of the MCM-41 nanoparticles was determined to be 192 ±1.782 nm on the basis of the findings of three separate particle size analyses as determined by dynamic light scattering (DLS), the results of which are shown in Figure 2. The size distribution of the MCM-41 nanoparticles was found to be within a narrow range, on the basis of the size distribution study results shown in Figure 2. According to BET analysis, the MCM-41 particles had a specific surface area of 1019.37 m2/g, a pore size of 2.42 nm, and a pore volume of 0.99 cm^3 g.

SEM analysis was used to examine the morphological structure of MCM-41. The SEM characterization results shown in Figure 3 revealed that the MCM-41 nanoparticles were nanosized, had a narrow size distribution, and were smooth, amorphous and spherical in shape. Additionally, SEM analysis, revealed that the images of the MCM-41

MEANDROS MEDICAL AND DENTAL JOURNAL
March 2025 (1): 12-18

Meandros Medical and Dental Journal
doi: 10.69601/meandrosmdj.1591566

nanoparticles (Figure 3-A) and APTES-coated MCM-41 nanoparticles (Figure 3-B) were similar.

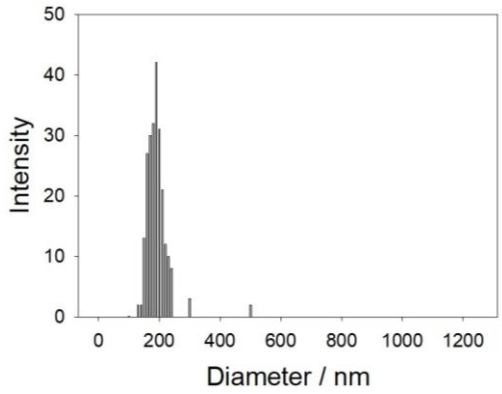

Figure 2. DLS particle size analysis of the MCM-41 nanoparticles

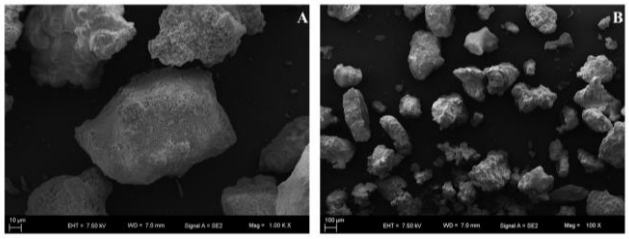

Figure 3. SEM images for morphological analysis of the MCM-41 nanoparticles (A), and APTES-coated MCM-41 nanoparticles (B).

Through an APTES reaction, MCM-41 nanoparticles (shown in Figure 4-A) were functionalized with amino groups (shown in Figure 4-B). FT-IR analysis was performed to determine the correct conjugation. The FT-IR study was performed in ATR mode with 3 replicates. Typical bands at 690 and 1460 nm, which correspond to N–H bending vibrations and N–H asymmetric bending vibrations, respectively, emerged following amino grafting, as shown in Figure 4-B.

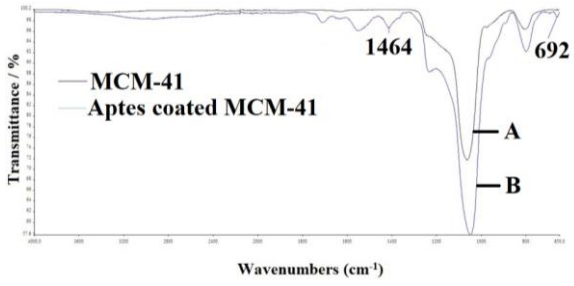

Figure 4. FTIR spectra of the MCM-41 nanoparticles (A), and APTES-coated MCM-41 nanoparticles (B).

The use of aptamer-functionalized silica magnetic nanoparticles for prepurification in a homogeneous test for the detection of *S. aureus* in PBS samples allowed for the elimination of interference from PBS. At detection limits as low as 164 CFU/mL in PBS, rapid and sensitive detection of *S. aureus* was obtained. Adsorption by electrostatic attraction between negatively charged oligonucleotides and the positively charged silica surface was used to achieve DNA capping.

In Figure 5, the green line shows fluorescein-loaded silica particles without aptamer and any target bacteria. The blue line shows fluorescein-loaded silica particles conjugated with the aptamer and the target bacterium *S. aureus*. The gray line shows fluorescein-loaded silica particles conjugated with the aptamer and the target bacteria *S. epidermidis*. The red line shows fluorescein-loaded silica particles conjugated with the aptamer without any target bacteria. The yellow line shows fluorescein-loaded silica particles conjugated with the aptamer and the target bacteria *E. coli*. The release of fluorescein was measured at various intervals. The standard deviation of experiments conducted in triplicate is shown by error bars.

The *S. aureus* aptamer blocked the silica nanoparticles after they were loaded with reporter fluorescein molecules. In the release experiments (Figure 5), minimal release of fluorescein was observed in the fluorescein-loaded silica particles conjugated with the aptamer without any target bacteria and in the fluorescein-loaded silica particles conjugated with the aptamer and the target bacteria *E. coli*. Fluorescein-loaded silica particles conjugated with aptamer and the target bacterium *S. epidermidis* also resulted in minimal release. The maximum release profile of fluorescein-loaded silica particles conjugated with the aptamer and the target bacterium *S. aureus* was similar to that of the positive control (fluorescein-loaded silica particles without the aptamer and any target bacteria). In addition, approximately 70% fluorescein release occurred within 6h.

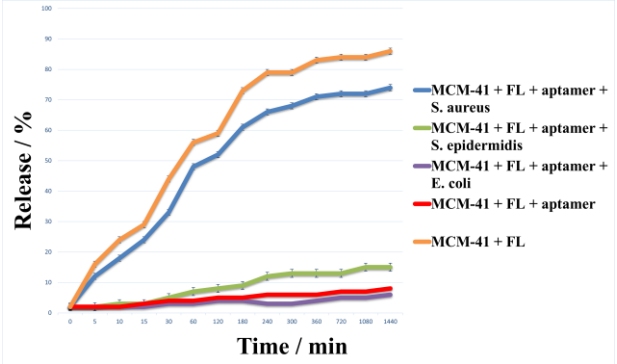

Figure 5. Fluorescein release profile from aptamer conjugated MCM-41 nanoparticles.

DISCUSSION

Numerous infections are caused by the important human pathogen *S. aureus*. For treatment and control to be effective, quick and precise detection techniques are essential. Recently, researchers have investigated how to use aptamer-gated nanoparticles to find *S. aureus*. This is possible because aptamers are very sensitive and specific (18).

The size range of MCM-41 nanoparticles is usually between 40 and 200 nm, and their size distribution is narrow, which makes them uniform (19, 20). Transmission electron microscopy and X-ray diffraction revealed that the nanoparticles had a smooth surface and a structure made of amorphous silica. The display of these characteristics of the nanoparticles (21) supports this finding. SEM, revealed that the majority of the nanoparticles that make up MCM-41 have a spherical shape (21, 22).

The band at 690 nm represents the N–H bending vibrations. This is a typical feature of hydrogen-bonded amino group infrared spectra, where anharmonic interactions couple the bending and stretching vibrations together. N-H asymmetric bending vibrations are linked to the band at 1460 nm. This band is made up of complex vibrational interactions inside the amino group, especially those involving asymmetric stretching and bending modes (23). In line with this study, Ercan and colleagues (24) reported that the bands that appeared in the FTIR analysis at approximately 690 and 1460 after amine functionalization are responsible for N–H bending vibrations and N–H asymmetric bending vibrations. The existence of these two bands was often regarded as proof of the presence of amino groups on the silica surfaces.

Using fluorescein-loaded silica particles linked with aptamers has been shown to be a successful way to target *S. aureus*. This strategy ensures sensitive and targeted detection and release, depending on the strong affinity of the aptamer for *S. aureus*. This study achieved rapid and sensitive detection of S. aureus, with detection limits as low as 164 CFU/mL in PBS. This study was similar to that of Shangguan et al., who used click chemistry to attach chloropropyl-functionalized fluorescent silica nanoparticles (FSiNPs) to aptamers that bind strongly to S. *aureus*. In microfluidic channels, this bioconjugate (Apt(*S.aureus*)/FNPs) enabled sensitive and rapid detection of *S. aureus*, with detection limits of 270 cfu/mL in spiked water samples and 93 cfu/mL in deionized water (25). Another study used a dual-color flow cytometry assay with aptamer/FSiNPs to show that *S. aureus* could be easily identified and fluorescently labeled, with limits of detection of 150 cells/mL in buffer and 760 cells/mL in spiked milk (26). They reported that *S. aureus* could be easily identified and fluorescently labeled, with limits of detection of 150 cells/mL in buffer and 760 cells/mL in spiked milk (26). Zhu and colleagues reported that signal molecules (4-aminothiophenol, 4-ATP) were placed on mesoporous silica nanoparticles (MSNs). Raman spectroscopy was used to detect the signal molecules after the aptamer gates opened upon binding to *S. aureus*. This method revealed a straight-line connection between the amount of *S. aureus* and the signal strength, with a detection limit of 17 cfu/mL (27).

Using aptamer-gated nanocapsules, Kavruk et al. reported that mesoporous silica nanoparticles could be used to target *S. aureus* for antibiotic delivery, which led to a specific decrease in the minimum inhibitory concentration (MIC) of vancomycin (28). Borsa and colleagues published a homogeneous test for *S. aureus* identification that uses aptamer-functionalized silica magnetic nanoparticles to prepurify blood samples. This method eliminates interference from blood components. This technique detected as few as 682 CFU of *S. aureus* in whole blood (29). Chen and colleagues reported that the fiber sensor they made can find *S. aureus* in PBS with a response time of less than 30 minutes and a limit of detection of 3.1 CFU/mL (30). He and colleagues reported that they used aptamer recognition and fluorescent silica nanoparticles to develop a sensitive and specific way to find *S. aureus*. This method can find as few as 1.5×10^2 cells/mL in buffer and spiked milk, which is much lower than Aptamer/FITC-based flow cytometry (31). In their study, Qiao and colleagues developed a new aptamer-based fluorometric assay that can quickly and accurately find methicillin-resistant *S. aureus* in clinical samples. Within two hours, methicillin-resistant *S. aureus* can be detected in clinical samples. It can find as few as 2.63×10^3 CFU/mL in PBS and 1.38×10^3 CFU/mL in spiked nasal swabs (32).

CONCLUSION

The proposed biosensor offers several advantages, including rapid response times, high sensitivity, and specificity for *S. aureus* detection. It can also work with different sample matrices and can be added to portable and automated platforms, which makes it a useful tool for onsite detection in a range of situations. This platform's unique properties make it an ideal candidate for many applications in healthcare and biotechnology.

Acknowledgments
The author expresses his gratitude to Prof. Dr. Veli Cengiz Özalp for his valuable insights and support.

Authorship contributions
S.U. was the designer of the study and contributed to every section of the article. The author reviewed and approved the final draft of the text.

Data availibity statement
Data will be made available on request.

Declaration of competing interest
The author declares that he has no conflict of interest.

Ethics
This study does not require ethical committee approval.

Funding
This research did not receive any specific grant from funding agencies in the public, commercial, or not-for-profit sectors.

REFERENCES
1. Liu A, Garrett S, Hong W, Zhang J. Staphylococcus aureus Infections and Human Intestinal Microbiota. Pathogens 2024; 13(4): 276.

2. Idrees M, Sawant S, Karodia N, Rahman A. Staphylococcus aureus biofilm: Morphology, genetics, pathogenesis and treatment strategies. Int J Environ Res Public Health 2021; 18(14): 7602.

3. Alves J, Vrieling M, Ring N, Yebra G, Pickering A, Prajsnar TK, Renshaw SA, Fitzgerald JR. Experimental evolution of Staphylococcus aureus in macrophages: dissection of a conditional adaptive trait promoting intracellular survival. mBio 2024; 15(6): e0034624.

4. Kavanagh KT. Control of MSSA and MRSA in the United States: protocols, policies, risk adjustment and excuses. Antimicrob Resist Infect Control 2019; 8: 103.

5. Qiu M, Zheng M, Zhang J, Yang X, Zhang Y, Zhang W, Man C, Zhao Q, Jiang Y. Recent advances on emerging biosensing technologies and on-site analytical devices for detection of drug-resistant foodborne pathogens. Trends Anal Chem 2023; 167: 117258.

6. García-Uriostegui L, Meléndez-Ortiz HI, Mata-Padilla JM, Toriz G. Fast fabrication of mesostructured MCM-41-type nanoparticles by microwave-induced synthesis. Ceram Int 2023; 49: 28693-28701.

7. Wei Y, Yang W, Yang Z. An excellent universal catalyst support-mesoporous silica: Preparation, modification and applications in energy-related reactions. Int J Hydrogen Energy 2022; 47(16): 9537-9565

8. Trzeciak K, Chotera-Ouda A, Bak-Sypien II, Potrzebowski MJ. Mesoporous silica particles as drug delivery systems-the state of the art in loading methods and the recent progress in analytical techniques for monitoring these processes. Pharmaceutics 2021; 13(7): 950.

9. Fu Z, Xiang J. Aptamer-functionalized nanoparticles in targeted delivery and cancer therapy. Int J Mol Sci 2020; 21(23): 9123.

10. Stoltenburg R, Reinemann C, Strehlitz B. Selex—a (r) evolutionary method to generate high-affinity nucleic acid ligands. Biomol Eng 2007; 24(4): 381-403.

11. Mairal T, Özalp VC, Sánchez PL, Mir M, Katakis I, O'Sullivan CK. Aptamers: Molecular tools for analytical applications. Anal Bioanal Chem 2008; 390: 989-1007.

12. Zhou H, Li Y, Wu W. Aptamers: Promising Reagents in Biomedicine Application. Adv Biol 2024; 8(6): 2300584.

13. Anarjan FS. Active targeting drug delivery nanocarriers: Ligands. Nano-Struct Nano-Objects 2019; 19: 100370.

14. Cao X, Li S, Chen L, Ding H, Xu H, Huang Y, Li J, Liu N, Cao W, Zhu Y, Shen B, Shao N. Combining use of a panel of ssdna aptamers in the detection of staphylococcus aureus, Nucl Acids Res 2009; 37(14): 4621-4628.

15. Borsa BA, Tuna BG, Hernandez FJ, Hernandez LI, Bayramoglu G, Arica MY, Ozalp VC. Staphylococcus aureus detection in blood samples by silica nanoparticle-oligonucleotides conjugates. Biosens Bioelectron 2016; 86: 27-32.

16. Ozalp VC, Eyidogan F, Oktem HA. Aptamer-gated nanoparticles for smart drug delivery. Pharmaceuticals 2011; 4(8): 1137-1157.

17. Ozalp VC, Schäfer T. Aptamer - based switchable nanovalves for stimuli - responsive drug delivery. Chem Eur J 2011; 17(36): 9893-9896.

18. Chen W, Lai Q, Zhang Y, Liu Z. Recent advances in aptasensors for rapid and sensitive detection of Staphylococcus aureus. Front Bioeng Biotechnol 2022; 10: 889431.

19. Castillo RR, de la Torre L, García-Ochoa F, Ladero M, Vallet-Regí M. Production of MCM-41 nanoparticles with control of particle size and structural properties: optimizing operational conditions during scale-up. Int J Mol Sci 2020; 21(21): 7899.

20. Jomekian A, Mansoori SAA, Monirimanesh N. Synthesis and characterization of novel PEO–MCM-41/PVDC nanocomposite membrane. Desalination, 2011; 276(1-3): 239-245.

21. Dau TAN, Le VMH, Pham TKH, Le VH, Cho SK, Nguyen TNU TKH, Van Tran, TT. Surface functionalization of doxorubicin loaded MCM-41 mesoporous silica nanoparticles by 3-aminopropyltriethoxysilane for selective anticancer 9 effect on A549 and A549/DOX cells. J Electron Mater 2021; 50: 2932-2939.

22. Khalil KMS. Cerium modified MCM-41 nanocomposite materials via a nonhydrothermal direct method at room temperature. J Colloid Interface Sci 2007; 315(2): 562-568.

23. Mishra S, Nguyen HQ, Huang QR, Lin CK, Kuo JL, Patwari GN. Vibrational spectroscopic signatures of hydrogen bond induced NH stretch–bend Fermi-resonance in amines: The methylamine clusters and other N–H··· N hydrogen-bonded complexes. J Chem Phys 2020; 153(19): 194301

24. Ercan M, Ozalp VC, Tuna BG. Genotyping of single nucleotide polymorphism by probe-gated silica nanoparticles. Anal Biochem 2017; 537: 78-83.

25. Shangguan J, Li Y, He D, He X, Wang K, Zou Z, Shi H. A combination of positive dielectrophoresis driven on-line enrichment and aptamer-fluorescent silica nanoparticle label for rapid and sensitive detection of Staphylococcus aureus. Analyst, 2015; 140(13): 4489-4497.

26. He X, Li Y, He D, Wang K, Shangguan J, Shi H. Aptamer-fluorescent silica nanoparticles bioconjugates based dual-color flow cytometry for specific detection of Staphylococcus aureus. J Biomed Nanotechnol 2014; 10(7): 1359-1368.

27. Zhu A, Jiao T, Ali S, Xu Y, Ouyang Q, Chen Q. SERS sensors based on aptamer-gated mesoporous silica nanoparticles for quantitative detection of Staphylococcus aureus with signal molecular release. Anal Chem 2021; 93(28): 9788-9796.

28. Kavruk M, Celikbicak O, Ozalp VC, Borsa BA, Hernandez FJ, Bayramoglu G, Salih B, Arica MY. Antibiotic loaded nanocapsules functionalized with aptamer gates for targeted destruction of pathogens. Chem comm 2015; 51(40): 8492-8495.

29. Borsa BA, Tuna BG, Hernandez FJ, Hernandez LI, Bayramoglu G, Arica MY, Ozalp VC. Staphylococcus aureus detection in blood samples by silica nanoparticle-oligonucleotides conjugates. Biosens Bioelectron 2016; 86: 27-32.

30. Chen L, Leng YK, Liu B, Liu J, Wan SP, Wu T, Yuan J, Shao L, Gu G, Fu Y, Xu H, Xiong Y, He X, Wu Q. Ultrahigh-sensitivity label-free optical fiber biosensor based on a tapered singlemode-no core-singlemode coupler for Staphylococcus aureus detection. Sens Actuators B Chem 2020; 320: 128283.

31. He X, Li Y, He D, Wang K, Shangguan J, Shi H. Aptamer-fluorescent silica nanoparticles bioconjugates based dual-color flow cytometry for specific detection of Staphylococcus aureus. J Biomed Nanotechnol 2014; 10(7): 1359-1368.

32. Qiao J, Meng X, Sun Y, Li Q, Zhao R, Zhang Y, Wang J, Yi Z. Aptamer-based fluorometric assay for direct identification of methicillin-resistant Staphylococcus aureus from clinical samples. J Microbiol Methods 2018; 153: 92-98.